

# Experimental Study of Power Exchange Using a Twin Spool Engine Emulator

Hossein Balaghi Enalou, Mohamed Rashed, Ponggorn Kulsangcharoen, Shajjad Chowdhury, Serhiy Bozhko

Department of Electrical and Electronic Engineering, Faculty of Engineering,

University of Nottingham, University Park, Nottingham, UK, NG7 2RD. Email: eexhb3@nottingham.ac.uk

**Abstract**— The More Electric Aircraft (MEA) nad , with electrical machines on both HP and LP shafts and the advancements in power electronics, makes it possible to transfer power electrically from one spool to another. Preliminary results have shown considerable improvement in turbofan performance in terms of fuel consumption, engine stability and compatible thrust with flight mission. In order to proof the concept of power exchange between shafts it is essential to design a subscale system to emulate the more electric engine (MEE). This paper describes the layout of the experimental system to emulate the MEE to study the idea of power exchange between shafts through a single dc bus architecture.

**Keywords**—Engine Emulator, power exchange, More Electric Aircraft (MEA)

## I. INTRODUCTION

The concept of the More Electric Aircraft (MEA) has resulted in introduction of various new technologies via advancements of on-board electrification. Successful achievement of these innovative ideas will mean development of new knowledge towards further reduction of aircraft weight, equipment volume, overall fuel burn and improved efficiency of aircraft systems, hence less environmental impact and greener aviation.

One of the main areas of the research for the MEA is on mounting a generator on the Low Pressure (LP) shaft in addition to the starter/generator on the High Pressure (HP) shaft of the engine [1].

Given that there are electrical machines on both LP and HP shafts, the authors of this paper have introduced the idea of power exchange between shafts in a single dc bus architecture in [2]. In this architecture, the alternating outputs of electrical machines are connected to a single dc bus through bidirectional convertors which helps dynamically controllable power transfer between the LP and HP shafts. The direction of power circulation, depending on flight mission to have the optimum performance of the engine, can be either from the LP shaft to the HP shaft, or from the HP shaft to the LP shaft or power split between the LP and HP shafts for the Electric Power System (EPS) of the aircraft. Preliminary results in [2] show great possible benefits in terms of fuel consumption, engine stability and compatible thrust with flight mission at various flight scenarios.

At the initial stage, in order to prove the concept and demonstrate the practicality of this idea, it is essential to design a subscale system to emulate the More Electric Engine (MEE). The engine emulator would enable better understanding and preliminary analysis of the idea of power circulation between shafts. Accordingly, it can closely

resemble the overall electrical energy generation system under various operating conditions experimentally without the need to operate the real engine.

Aspects such as electric machine and power converter topologies, electric power quality, Fault scenarios on the performance of the new architecture, regeneration management, as well as the overall center safety, reliability and availability will be thoroughly investigated.

Such an integrated power center can be designed to provide optimized operation according to the Engine Operation Mode (EOM) with simultaneous minimization of overall weight and volume, increasing the overall system efficiency, as well as improving its reliability and maintainability.

In the literature, aero-derivative gas turbine engine emulation has been widely implemented in the Hardware in the Loop (HIL) environment [3]-[5]. HIL simulation provides the ability to study the system in a safe and controlled fashion [6].

In this paper, an HIL simulation framework is developed for the power system of the aircraft. This will consider the engine as a part of the overall electrical energy generation system, together with the driven generators, one from the LP shaft and another one from the HP shaft, and the power electronic converters controlling the generation.

For this purpose, a twin spool turbofan real-time model is downloaded into the dSPACE control system for the Hardware in the Loop (HIL) implementation. The engine's HP and LP shaft speed set-points, generated by dSPACE, are sent to two drives to mimic the speed-torque characteristic of the turbofan shafts. Drives are controlling two standard induction machines which are coupled with the state-of-the-art engine electrical machines by shafts. The alternating outputs of these machines are connected to a single dc bus through bidirectional converters. Power can be transferred between engine shafts through the dc bus which will be also connected to programmed EPS in future.

The paper is organized as follows: Section II gives a brief introduction into the idea of electrical power transfer. Section III describes the emulation system. In Section IV the theory of similarity is exemplified. Section V presents the engine model and its control system used for the emulator and Section VI concludes the paper.

## II. ELECTRIC POWER TRANSFER BETWEEN SHAFTS

The LP and HP shafts of the engine are not connected mechanically, however their speeds are thermodynamically

coupled which imposes certain operational constraints specifically at the engine low speed settings. For this reason, there will be a great interest in controllable power transfer between shafts to decouple shaft speeds relatively depending on the amount of power transfer.

MEA can provide this possibility since electrical machines are connected to both LP and HP shafts through fixed speed ratio gearboxes. A well-known architecture for the MEA is the single dc bus architecture, widely elaborated in the literature [7]-[9], within which the machine outputs are connected to the dc bus through bidirectional convertors, shown in Fig. 1. This provides the opportunity to circulate dynamically controllable power between shafts through electrical machines by power electronics privilege.

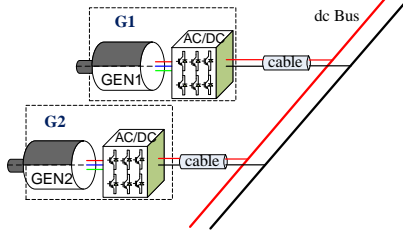


Fig. 1. Configuration of single dc bus multi-source EPS

This configuration accommodates the engine with flexible power split ratios at different operational speeds depending on the amount of power transfer. The power circulation between shafts can simply be expressed as below:

$$T_{ELP} \times \omega_{LP} + T_{EHP} \times \omega_{HP} + P_{EPS} + P_{loss} = 0 \quad (1)$$

where  $T_{EHP}$  and  $T_{ELP}$  are the torques on the electrical machines connected the HP and LP shafts respectively with the corresponding speeds of  $\omega_{HP}$  and  $\omega_{LP}$ .  $P_{EPS}$  is the load on the dc bus from the EPS and  $P_{loss}$  is the power loss in the system.

### III. GAS TURBINE ENGINE EMULATION SYSTEM

To investigate the power transfer effect between the HP and LP shafts on the aircraft engine performance, the aircraft engine emulator system is constructed. The emulator system shown in Fig. 2 comprises of two Oswald induction machines with two front-end 40 kW drives and a dSPACE Rapid Controlled Prototyping (RCP) system. The system can deliver peak power of 50 kW per shaft. The drives control the induction machines to mimic the HP and LP engine prime-movers' characteristics, which have wide speed range from 10000 to 20000rpm, considering the gear ratios for the generators on the LP and HP shafts.

On the emulator test bed, as illustrated in Fig. 3, an AEGART Permanent Magnet Synchronous Machine (PMSM) and a Switched-Reluctance Machine (SRM) are connected to the

LP and HP shafts' drives respectively. The alternating outputs of both machines are connected to the aircraft DC power system through bidirectional power converters.

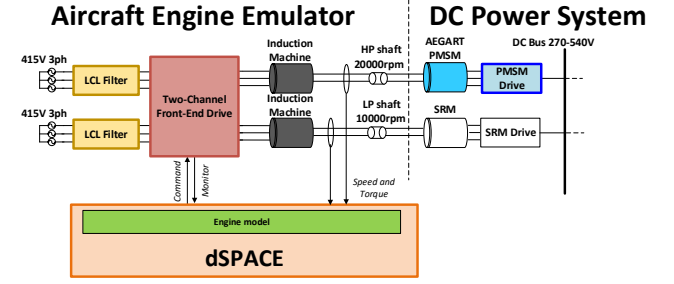


Fig. 2. The emulator system layout

The dSPACE control platform is employed in order to have high flexibility in implementing and updating the complex nonlinear aircraft engine model. The engine model simulink block diagram design is automatically implemented into dSPACE to be calculated in real time. It receives torque measurements from both shafts and produces speed references to the drives. The drives have their own fast speed control loop (i.e. current control loop) and are front-end type so they can straightforwardly regenerate power back to the grid.

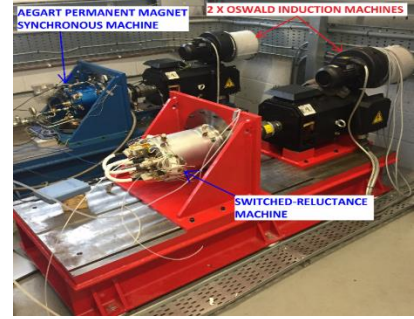


Fig. 3. The emulator HP and LP testbeds

### IV. SIMILARITY ANALYSIS

For the studied engine in [2], the amount of power transfer between shafts has been considered to be around 500 kW. However, the nominal power of electrical machine for the designed emulator is 50 kW. In this case either the engine model or the electrical system should be scaled to make the emulation compatible with the real system performance. Due to complexity of the engine model, electrical power system is scaled using similarity rules in [10]. To exemplify, the PMM is scaled as below.

The dynamic equations for PM machine in dq frame are:

$$L_d \frac{di_d}{dt} = v_d - Ri_d + L_q p \omega_r i_q \quad (2)$$

$$L_q \frac{di_q}{dt} = v_q - Ri_q - (L_d p \omega_r i_d + \phi_m p \omega_r) \quad (3)$$

where:  $v_d$ ,  $v_q$ ,  $i_d$  and  $i_q$  are the d and q-axis voltage and current components and the positive current is the current

following into the machine.  $R_s$ ,  $L_d$  and  $L_q$  are the stator resistance and inductances,  $\omega_r$  is the mechanical rotor speed,  $p$  is the number of pole pairs and  $\phi_m$  is the permanent magnet flux.

Dividing equations (2) and (3) respectively by  $Ri_d$  and  $Ri_q$ , the equations below are obtained,

$$1 + \frac{L_d}{Ri_d} \frac{di_d}{dt} - \frac{v_d}{Ri_d} - \frac{L_q p \omega_r i_q}{Ri_d} = 0 \quad (5)$$

$$1 + \frac{L_q}{Ri_q} \frac{di_q}{dt} - \frac{v_q}{Ri_q} + \frac{L_d p \omega_r i_d + \phi_m p \omega_r}{Ri_q} = 0 \quad (6)$$

Considering two PMM, since the phenomena are similar, the parameters can be related by scale factors ( $m$ ) as below:

$$t_1 = m_t t_2, R_1 = m_R R_2, \dots \quad (7)$$

The same is applied for  $L$ ,  $p$ ,  $\phi_m$ ,  $v_d$ ,  $v_q$ ,  $i_d$  and  $i_q$ .

By substituting (7) into (5) and (6), the equations below are obtained:

$$1 + \frac{m_L}{m_R m_t} \frac{L_{d2}}{R_{2i_{d2}}} \frac{di_{d2}}{dt_2} - \frac{m_{L_q} m_p m_{\omega_r} m_{i_q}}{m_R m_{i_d}} \frac{L_{q2} p_2 \omega_{r2} i_{q2}}{R_{2i_{d2}}} - \frac{m_{v_d}}{m_R m_{i_d}} \frac{v_{d2}}{R_{2i_{d2}}} = 0 \quad (8)$$

The same is applied for q axis equation. Since equations (5) and (6) are homogeneous, from equations (8), it can be found out that the scale factors are related as below:

$$1 = \frac{m_{v_d}}{m_R m_{i_d}} = \frac{m_{L_q} m_p m_{\omega_r} m_{i_q}}{m_R m_{i_d}} = \frac{m_L}{m_R m_t} = \frac{m_{v_q}}{m_R m_{i_q}} = \frac{m_{L_d} m_p m_{\omega_r} m_{i_d}}{m_R m_{i_q}} = \frac{m_{\phi_m} m_p m_{\omega_r}}{m_R m_{i_q}} \quad (9)$$

Replacing the scale factors by the ratios of corresponding parameters, the relation below is obtained:

$$\frac{v_{d1}/v_{d1}}{(R_1/R_2)(i_{d1}/i_{d1})} = 1, \dots \quad (10)$$

In the notation for general similarity criteria:

$$\pi_1 = \frac{v_d}{Ri_d}, \pi_2 = \frac{v_q}{Ri_q}, \pi_3 = \frac{L}{Rt}, \pi_4 = \frac{Lp\omega_r i_q}{Ri_d}, \pi_5 = \frac{\phi_m p \omega_r}{Ri_q} \quad (11)$$

Table I shows the specifications of the PMM used on the emulator rig (AEGART II) and a typical 500 kW PMM.

Table I Specifications of PMMs

Parameter	Symbol	Model (1)	Experiment (2)
Power rating	P	500 kW	50 kW
Phase resistance	$R_s$	0.38 mΩ	1.06 mΩ
Machine inductance	$L_d, L_q$	50 μH	99 μH
Permanent magnet flux linkage	$\phi_m$	0.060 $\frac{Vs}{rad}$	0.036 $\frac{Vs}{rad}$
Number of pole pairs	$p$	8	3
Speed	$\omega$	12000 rpm	20000 rpm
DC bus voltage	$V_{DC}$	540 volt	270 volt

The dependent values must be taken at corresponding moments of time. In the present case, those moments of time are in a way that:

$$t_1 = 1.4 t_2 \quad (12)$$

Which means 50 kW machine is 15 times faster than 500 kW machine. If machine independent parameters are assumed not to change by time, then the relations below between two machines are obtained:

$$\frac{v_{d1}}{i_{d1}} = 0.36 \frac{v_{d2}}{i_{d2}}, \frac{v_{q1}}{i_{q1}} = 0.36 \frac{v_{q2}}{i_{q2}}, \dots \quad (13)$$

## V. ENGINE MODEL

The Inter Component Volume (ICV) method has been implemented in the MATLAB/SIMULINK environment to develop a modulated multi-spool turbfan model in [11] which has been verified in [12].

Fig. 4 illustrate the arrangement of the engine component where  $\dot{m}$ ,  $T$ ,  $p$ ,  $\omega$  and  $P$  are mass flow, temperature, pressure, rotor speed and power respectively.

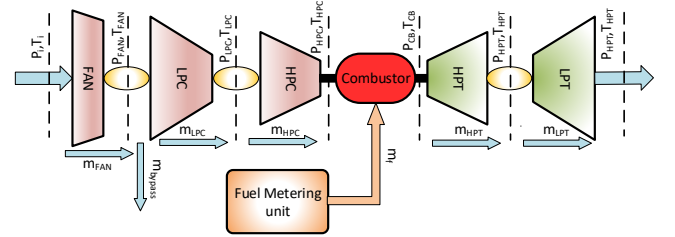


Fig. 4. Illustration of Jet-engine 0-dimensional component level model

A bump-less override control structure has also been implemented for the turbfan with limit controllers for over-temperature, surge and bleeding pressure for the Environmental Control System (ECS).

Shaft dynamics for the real system can be expressed as below:

$$T_{HPT} - T_{HPC} - J_{HP} \dot{\omega}_{HP} = T_{EHP} \quad (14)$$

$$T_{LPT} - T_{FAN} - T_{LPC} - J_{LP} \dot{\omega}_{LP} = T_{ELP} \quad (15)$$

where  $T_{HPT}$  and  $T_{LPT}$  are the generated torque by the High and Low Pressure Turbines (HPT and LPT) respectively,  $T_{HPC}$  and  $T_{LPC}$  are the consumed torque by the High and Low Pressure Compressors (HPC and LPC) respectively.

For the application in the emulator, component modules shown in Fig. 4Fig. 5 are solved online to provide  $T_{HPT}$ ,  $T_{LPT}$ ,  $T_{HPC}$  and  $T_{LPC}$  for the LP and HP shaft modules. The outputs of the engine model to the drives are LP and HP shafts real-time speed references while the inputs to the engine model are torque values of SR and PM machines corresponding to LP and HP shafts respectively.  $T_{EHP}$  and  $T_{ELP}$  are the signals from the torque sensors on emulator shafts after scaling.

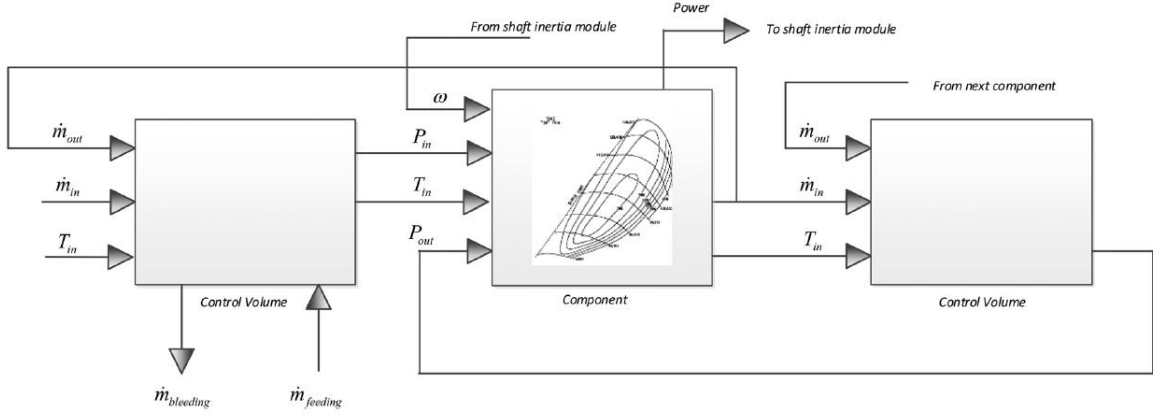


Fig. 5. Structure of gas turbine model component modules

The real-time outputs of shaft dynamic modules after solving equations (14) and (15) are the HP shaft speed,  $\omega_{HP}$ , and the LP shaft speed,  $\omega_{LP}$ , which, after scaling, are the speed references for the drives on the emulator rig.

## VI. REAL-TIME EMULATION

As discussed in section IV, the machined are scaled down from 500 kW to 50 kW which are shown in Fig. 6.

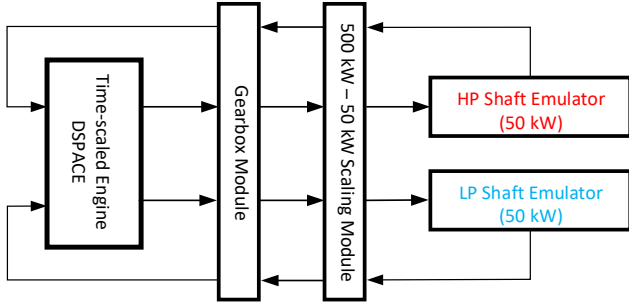


Fig. 6. Schematic of emulator rig simulation modules

Shaft emulators are inevitably in real-time and DSPACE runs the engine model in real time as well. While based on equation (12) the engine model simulation time should be scaled. If the real time is symbolised as  $t$ , since the emulator rigs run at real time then,  $t_2 = t$  and  $t_1 = m_t t$ . For the ICV approach, the state space vecetor/matrix differential equation gives:

$$\begin{aligned} \frac{dX_1}{dt_1} &= A(X_1).X_1(t_1) + B(X_1).U_1(t_1) \\ Y_1 &= C(X_1).X_1(t_1) + D(X_1).U_1(t_1) \end{aligned} \quad (16)$$

where  $X$  is the states' vector,  $U$  is the model input and  $Y$  is the model output and  $A$ ,  $B$ ,  $C$  and  $D$  are state dependent matrixes. For the second system with inputs,  $U_2$ , since the processes are similar,

$$X_1 = m_X X_2, U_1 = m_X U_2, t_1 = m_t t \quad (17)$$

Substituting (17) into (16), the state space equation in real time will be:

$$\begin{aligned} \frac{m_X dX_2}{m_t dt} &= A(m_X X_2).m_X X_2(t) + B(m_X X_2).m_U U_2(t) \\ m_Y Y_2 &= C(m_X X_2).m_X X_2(t) + D(m_X X_2).m_U U_2(t) \end{aligned} \quad (18)$$

As stated before, the engine model is preferred not to be scaled, for which:

$$m_X = m_U = m_Y = 1 \quad (19)$$

while the states corresponding to shaft speeds will be scaled separately with scale factor,  $M_N$  and the torque inputs to the engine will be scaled with the scale factor,  $M_T$ , to match real engine performance. As a result the state space equations will be scaled only in time as below:

$$\begin{aligned} \frac{dX_2}{dt_2} &= m_t (A(X_2).X_2(t) + B(X_2).U_2(t)) \\ Y_2 &= C(X_2).X_2(t) + D(X_2).U_2(t) \end{aligned} \quad (20)$$

In order to implement the time scaling shown in equation (20) in the ICV approach, the time scale factor block,  $m_t$ , is added before each state derivative in Simulink as shown in Fig. 7.

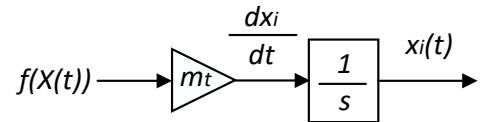


Fig. 7. Time scale block for Simulink state blocks

$X$  is the state vector and  $x_i$  is the corresponding state. Given that shaft speeds are states as well and  $J$  is the shaft inertia of the engine, applying the time scale  $m_t$  basically can be interpreted as that the inertia of the shafts are modified to  $\frac{J}{m_t}$ . It should be noted that model inputs which are a function of time such as throttle, should be scaled in time as well.

## VII. SIMULATION RESULTS

### A. Power off-take (real application)

For the existing EPS architectures with the starter/generator connected to the HP shaft, the amount of power off-take for a 140 kN turbofan is around 50 kW. Basically, AEGART has been designed to be mounted on the HP shaft of an aircraft engine HP shaft with approximately the same thrust rate as a starter/generator with the gear ratio of 1.

In order to study the performance of AEGART and its corresponding engine, the HP emulator rig can be used while  $m_t = 1$ .

Fig. 8 shows the speed tracking performance in which induction machine resembles the behavior of the engine shaft for the coupled PMM for a 40 % drop in throttle (at  $t=10s$ ) and then a rise at ( $t=20s$ ).

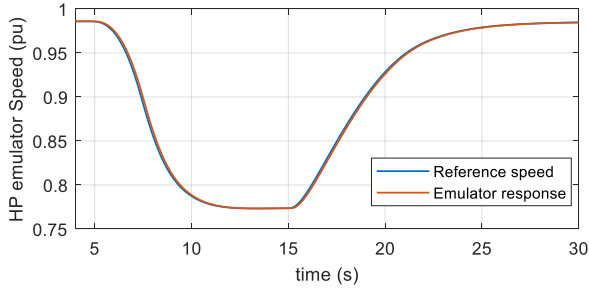


Fig. 8. Speed tracking of HP shaft emulator (engine transient,  $m_t = 1$ )

Fig. 9 shows the IM torque as a fraction of rated torque applied on emulator shaft in order to resemble the engine speed reference.

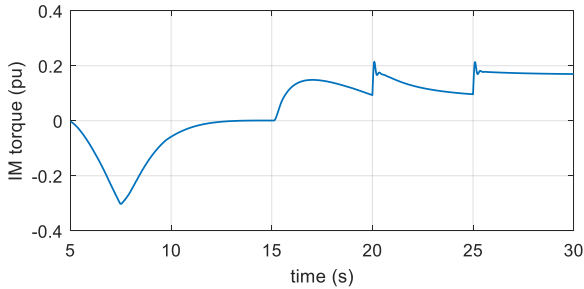


Fig. 9. IM torque (engine transient,  $m_t = 1$ )

Fig. 10 shows that PMM q-axis controller keeps the DC bus voltage at 270 volts during extracting power from HP shaft for the steps of 10 and 20 kW (shown in Fig. 11).

The power off-take shown in Fig. 12Fig. 10 is simulated during descent phase of the flight at 30000ft for which the speed tracking of the emulator is shown on Fig. 12. As it can be observed Speed tracking error during power off-take is less than 0.1 %.

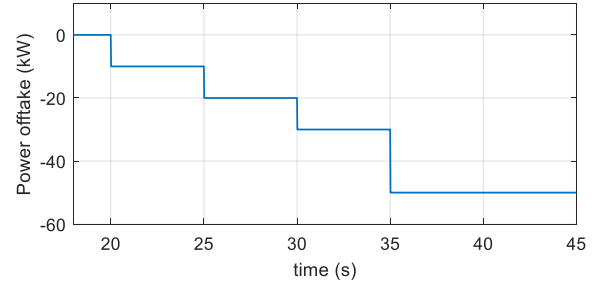


Fig. 10. Power off-take from HP shaft

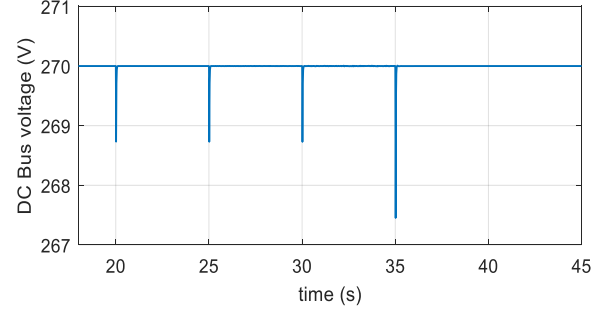


Fig. 11. DC bus voltage during power off-take

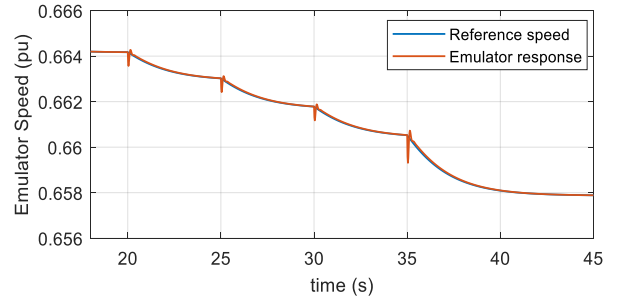


Fig. 12. Speed tracking of the emulator during power off-take

### B. Power transfer (similarity analysis)

This section presents the performance plots of key dynamic and steady-state tests. Maps from GASTURB have been used to model a two-spool high bypass ratio (BPR=8) unmixed flow 140 kN turbofan.

IM and PMM have been modeled in dq frame with a functional model for their convertors, while a switching model in PLECS has been implemented for the SRM in Simulink environment.

For the emulation SRM will be in motor mode and PMM will be in generation mode, while the speed of both machines is controlled by the induction machines coupled with them. Vector control scheme is implemented in order to control the speed of induction machines with bandwidth of 50 Hz. PMM controls the voltage of DC link which is 270V according to standard MIL-STD-704F with bandwidth of 100 Hz. For the

SRM, a torque control loop determines the amount of torque transfer from the LP to the HP shaft.

Table II shows the design speed of engine and electrical machine shafts.

Table II Design speed of engine and electrical machine shafts

	Engine (0)	500 kW machines (1)	50 kW machine (2)
LP (PM)	4000 rpm	12000 rpm	20000 rpm
HP (SRM)	18000 rpm	18000 rpm	12000 rpm

Accordingly, table III provides the gear ratio between the engine shafts and 500 kW electrical machine mounted on the engine,  $m_{gear} = \frac{\omega_1}{\omega_0}$ , the speed scale factor from the 500 kW electrical machine shafts to the PMM and SRM emulator shafts,  $m_\omega = \frac{\omega_1}{\omega_2}$  and their torque scale factors,  $m_T = \frac{T_1}{T_2}$ , from the emulator to the engine for the HP and LP shafts. Considering the amount of power scale from 500 kW to 50 kW;

$$\frac{P_1}{P_2} = \frac{T_1 \omega_1}{T_2 \omega_2} \quad (21)$$

by using the speed and power data from Table II,  $m_T$  can be calculated as below,

$$\text{for PMM; } m_T = \frac{T_1}{T_2} = \frac{500 \text{ kW}}{50 \text{ kW}} \times \frac{20000 \text{ rpm}}{12000 \text{ rpm}} = 16.67$$

$$\text{for SRM; } m_T = \frac{T_1}{T_2} = \frac{500 \text{ kW}}{50 \text{ kW}} \times \frac{12000 \text{ rpm}}{18000 \text{ rpm}} = 6.67$$

The time scale between the 500 kW machines and 50 kW machines is also  $m_t = 1.4$ .

Table III Gear and scaling ratios for the LP and HP shafts

	$m_{gear}$	$m_\omega$	$m_T$
LP (PMM)	3	0.6	16.67
HP (SRM)	1	1.5	6.67

The simulation block for the gear ratio and scale factors for speed and torque between the engine and the emulator rigs is shown in Fig. 13. A communication delay between the RTP and the emulator drive system has also been considered in the model.

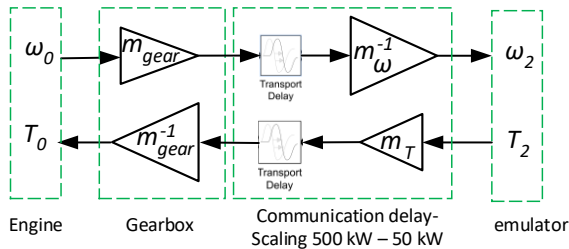


Fig. 13. Speed and torque communication between DSPACE and the emulator rig

The results depicted in **Error! Reference source not found.**Fig. 14 and **Error! Reference source not found.**Fig.

15 are the speed tracking performance of the emulator under rapid acceleration and deceleration of the engine between 50 % and 100 % of throttle.

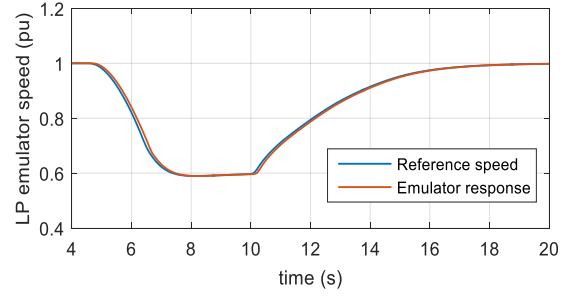


Fig. 14. Speed tracking of LP shaft emulator (engine transient,  $m_t = 1.4$ )

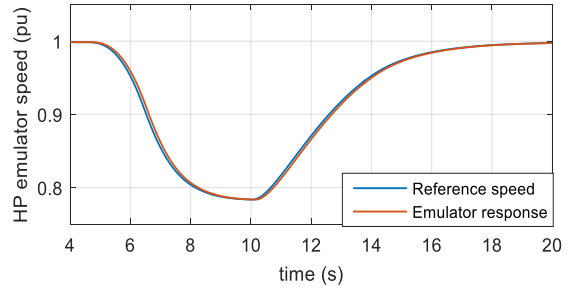


Fig. 15. Speed tracking of HP shaft emulator (engine transient,  $m_t = 1.4$ )

Fig. 16 and Fig. 17 show the IM torques as a fraction of rated torque applied on HP and LP emulator shafts respectively.

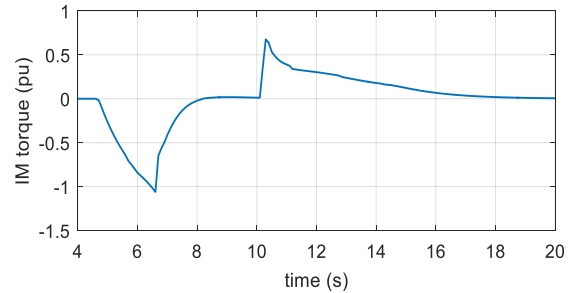


Fig. 16. LP emulator shaft IM torque (engine transient,  $m_t = 1.4$ )

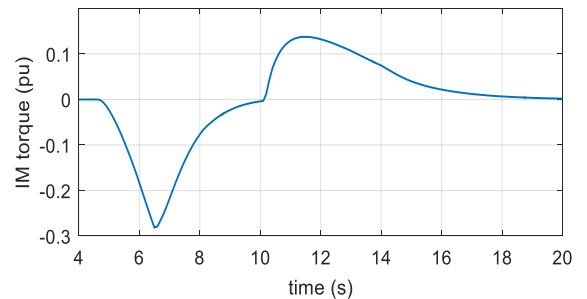


Fig. 17. HP emulator shaft IM torque (engine transient,  $m_t = 1.4$ )



## VIII. CONCLUSION

This paper has introduced an emulator for a turbofan engine which has been designed for use with a future integrated power center. The emulator will allow proving the idea of power exchange between the engine shafts conceptually. Simulation results of the whole emulation system in MATLAB/SIMULINK environment shows the facts that the emulator can closely mimic the overall electrical energy generation system under various operating conditions without the need to operate the real engine.

For future work, the engine emulator will be used in conjunction with a programmed aircraft EPS to investigate the engine interactions and control of Electric Power System (EPS), energy storage integration and optimized operation depending on Engine Operating Mode (EOM).

## IX. REFERENCES

- [1] M. J. Provost, "The More Electric Aero-engine: a general overview from an engine manufacturer," in *Power Electronics, Machines and Drives (PEMD2002)*, International Conference on (Conf. Publ. No. 487), 2002, pp. 246-251.
- [2] H. Balaghi Enalou, S. Bozhko, M. Rashed, P. Kulsangcharoen, "A Preliminary Study into Turbofan Performance with LP-HP Power Exchange", *GPPS Montreal 18 Proceedings, Global Power and Propulsion Society*.
- [3] B. A. Correa, Y. Zhang, R. A. Dougal, T. Chiocchio, K. Schoder, "Mechanical power-hardware-in-the-loop: Emulation of an aeroderivative twin-shaft turbine engine", *Proc. IEEE Electric Ship Technologies Symp.*, pp. 464-468, 2013.
- [4] Chengwei Gan, Rebecca Todd, Judith Apsley, "Mitigating Time Delays: An Evaluation of Their Impact Using a Simulation Model of an Aircraft Power System Demonstrator Facility", *Industry Applications Magazine IEEE*, vol. 21, pp. 44-53, 2015, ISSN 1077-2618.
- [5] M. Bash, M. Boyd and C. Miller, "Transient Engine Emulation within a Laboratory Testbed for Aircraft Power Systems", *SAE International Journal of Aerospace*, vol. 7, pp. 191, 2014, ISSN 1946-3901.
- [6] M. Montazeri-Gh and M. Nasiri, "Hardware-in-the-loop simulation for testing of electro-hydraulic fuel control unit in a jet engine application",
- [7] F. Gao, and S. Bozhko, "Modeling and Impedance Analysis of a Single DC Bus-Based Multiple-Source Multiple-Load Electrical Power System," *IEEE Transactions on Transportation Electrification*, 2017, vol. 2, PP. 335-346, issue. 3.  
doi:10.1109/TTE.2016.2592680
- [8] F. Gao, S. Bozhko, G. Asher, and P. Wheeler, "Comparative Study of Power Sharing Strategies for the DC Electrical Power System in the MEA," *SAE Technical Paper 2015-01-2410*, 2015, doi:10.4271/2015-01-2410.
- [9] F. Gao, S. Bozhko, G. Asher, P. Wheeler, and C. Patel, "An Improved Voltage Compensation Approach in a Droop-Controlled DC Power System for the More Electric Aircraft," *IEEE Transactions on Power Electronics*, 2016, vol. 31, pp. 7369-7383.
- [10] V. A. Venikov, Theory of similarity and simulation: with applications to problems in electrical power engineering, *Macdonald & Co., 1969*.
- [11] H. Balaghi Enalou, M. Rashed, P. Kulsangcharoen, C. I. Hill, and S. Bozhko, "Nonlinear aircraft engine model for future integrated power center development," *2016 ESARS-ITEC*, Toulouse, pp. 1-5.  
doi: 10.1109/ESARS-ITEC.2016.7841400
- [12] H. Balaghi Enalou, E. Abbasi Soreshjani, M. Rashed, S. Shen Yeoh, and S. Bozhko, "A Detailed Modular Governor-Turbine Model for Multiple-Spool Gas Turbine With Scrutiny of Bleeding Effect," *ASME. J. Eng. Gas Turbines Power*, 2017;139(11):114501-114501-6.  
doi:10.1115/1.4036947.